

Lawrence Berkeley National Laboratory

LBL Publications

Title

Elasticity, strength, and refractive index of argon at high pressures

Permalink

<https://escholarship.org/uc/item/3nd1c33b>

Authors

Chen, Bin
Gleason, A. E.
Yan, J. Y.
et al.

Publication Date

2010-04-14

Elasticity, strength, and refractive index of argon at high pressures

Bin Chen,^{1,2,*} A. E. Gleason,¹ J. Y. Yan,^{1,2} K. J. Koski,³ Simon Clark,^{1,2} and Raymond Jeanloz¹

¹Earth and Planetary Science, University of California–Berkeley, Berkeley, California 94720, USA

²Advanced Light Source, Lawrence Berkeley National Laboratory, Berkeley, California 94720, USA

³Chemistry Department, University of California–Berkeley, Berkeley, California 94720, USA

(Received 14 October 2009; revised manuscript received 9 March 2010; published 14 April 2010)

High-pressure Brillouin spectroscopy of polycrystalline argon, measured using two scattering angles (180° and 70°), determines the isotropic elastic moduli, shear strength, equation of state, and refractive index of face-centered-cubic argon from 1.3 to 30 GPa at room temperature. The index of refraction $n=1.33\text{--}1.67$ over this pressure range. An Eulerian finite-strain analysis (Birch-Murnaghan equation of state) yields an isothermal bulk modulus and pressure derivative $K_T=15.1(\pm 1.1)$ GPa and $K_T'=5.4(\pm 0.3)$ at 2 GPa. The resulting equation of state agrees well with previous x-ray diffraction measurements, illustrating the suitability of high-pressure Brillouin scattering for characterizing the elasticity and strength of polycrystalline materials.

DOI: 10.1103/PhysRevB.81.144110

PACS number(s): 62.20.de, 64.30.-t, 78.35.+c

I. INTRODUCTION

Brillouin spectroscopy is an important tool for determining the acoustic velocities, hence elastic moduli, of samples at high pressure.¹ Most prior work has focused on single crystals, yet there is significant interest in characterizing polycrystalline materials because of the difficulty in retaining single crystals over a broad range of pressures and temperatures, or through phase transitions; also, it has—so far—been impossible to synthesize certain materials as single crystals (e.g., Refs. 2–5).

Here we document the use of Brillouin scattering to characterize the index of refraction, equation of state and elastic moduli of fcc argon that is (meta-) stable between 1.3 and ~ 50 GPa at room temperature.⁶ Being a “noble gas” solid, Ar is of fundamental interest in physics and chemistry, and it is also of practical importance as a quasihydrostatic medium for high-pressure experiments.^{7–13} Our objective is to expand on two previous high-pressure Brillouin studies that are in partial agreement with each other.^{10,11}

II. EXPERIMENTAL

Gaseous argon ($>99.9\%$ purity) was cooled using liquid nitrogen and loaded as liquid in a gasketed symmetric diamond-anvil cell along with 3–5 ruby spheres (≤ 5 μm diameter) serving as pressure calibrants.¹⁴ The diamond culets were 300 μm across and the sample chamber consisted of a 100- μm -diameter hole drilled through a rhenium foil of 250- μm initial thickness, preindented to 44 μm . Using x-ray diffraction, we confirmed the fcc structure and polycrystalline nature of our argon sample at 4 GPa and room temperature. Crystal sizes were visually observed to be in the range $\sim 2\text{--}10$ μm .

Brillouin spectra were collected using a six-pass tandem (Sandercock) Fabry-Perot interferometer with confocal optics.¹⁵ A 532 nm Nd:YVO₄ laser (2 W maximum power) acts as probe and a fluorescence spectrometer integrated into the Brillouin system allows *in situ* pressure measurements to be made without moving the sample. The probe laser is polarized and can be focused to a ~ 20 μm diameter spot in the

sample at high pressures; both 180° and 70° scattering geometries can be collected without moving the sample (Fig. 1). We did not observe peak shapes characteristic of multiple elastic scattering, presumably because all of our spectra were collected at elevated pressures.¹⁶

III. RESULTS AND DISCUSSION

Both transverse (shear) and longitudinal (compressional) modes appear in spectra collected in transmission. If an equal-angle geometry is used with a parallel-sided sample (scattering angle $\theta=70^\circ$ in the present case), the index of refraction of the sample does not need to be known: the wave velocity is related to the Brillouin frequency shift (Ω) by $V=\lambda\Omega/[2\sin(\theta/2)]$.¹⁷ In comparison, spectra collected from

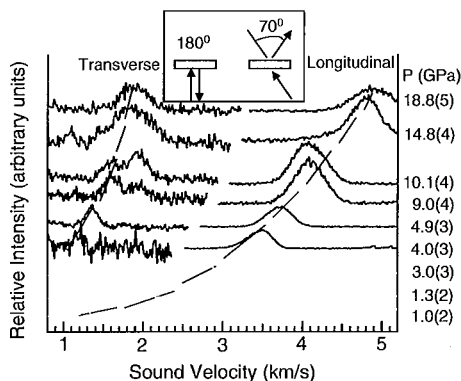


FIG. 1. Representative Brillouin spectra of polycrystalline argon collected as a function of pressure at room temperature: only parts of the 70° scattering patterns are shown, the spectra in grey are collected on decompression (all others are on compression), and the dashed curves are guides indicating the pressure shifts of individual modes. As evident from the signal/noise ratios, intensities of the transverse modes are about one order of magnitude lower than those of the longitudinal modes, consistent with the elasto-optical coefficients of crystalline Ar measured at zero pressure and 82 K (Refs. 20 and 21). Inset: schematic of scattering geometries used in the present study.

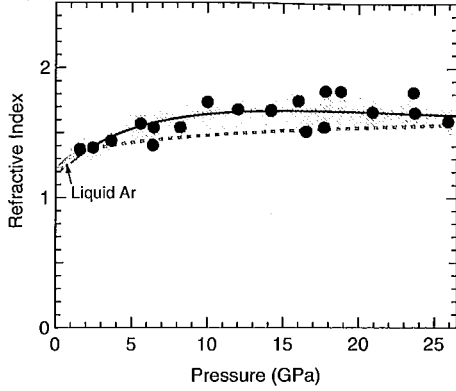


FIG. 2. Refractive index (n) of fcc argon obtained from Brillouin spectra with individual points indicating results from a given sample and pressure obtained at two different scattering angles (fit and uncertainty are shown by the solid line and shading, respectively). Liquid values are indicated by grey symbols (Ref. 9) and the dashed line gives the model values used in Ref. 10.

polycrystalline samples in backscatter ($\theta=180^\circ$) geometry typically have greater signal-to-noise ratio but only the longitudinal mode is present and the index of refraction of the sample must be known to determine the wave velocity from the frequency shift [$V=\lambda\Omega/(2n)$].

By collecting spectra in the two geometries, we determine both transverse (V_S) and longitudinal (V_P) wave velocities, as well as n as a function of pressure.¹⁷⁻¹⁹ We obtain the refractive index from $n=(\Omega_{180}/\Omega_{70})\sin(35^\circ)$, finding that it ranges from about 1.33–1.67 over the pressure range of our measurements and that it is in good accord with the results of previous studies on liquid Ar at room temperature (Fig. 2).^{9,10} This agreement provides independent validation of our velocity measurements at low pressure and our measurements allow us to correct Grimsditch *et al.*'s⁹ estimated index of refraction values for pressures up to 25 GPa (Fig. 2).

We did not observe hysteresis in longitudinal or shear velocities measured on compression and decompression (Figs. 1 and 3). However, this conclusion requires clarification because a considerable range of velocities is observed at a given pressure, depending both on the location of the probing laser beam within the sample and on rotation (chi angle) of the sample about the loading (and optical) axis of the diamond cell (Fig. 3). Part of the observed scatter may be due to pressure variations across the sample but this contribution is small relative to variations due to the dependence of wave velocities on direction through individual crystals. This conclusion is supported both by the orientation dependence of velocities at a given point—effectively, at a single pressure—in the sample (Fig. 3), and by comparing the velocity variations against the (modest) pressure variations measured across the sample. The scatter in velocities is reproducibly measured at ≥ 4 spots for a given sample and pressure, and is typically more than five to ten times the resolution in the frequency shifts of the Brillouin peaks.

Therefore, the observed scatter should not be treated as an “error” in the measurements but as reflecting orientation dependencies of acoustic velocities and corresponding orienta-

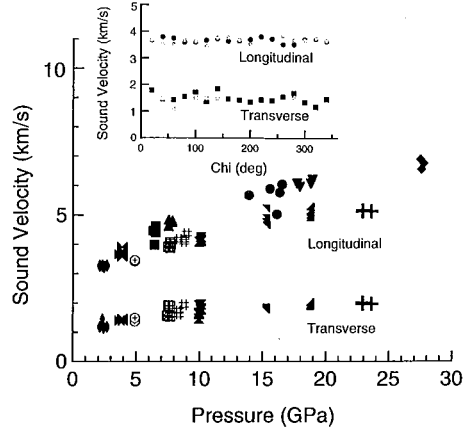


FIG. 3. Longitudinal (V_P) and transverse (V_S) acoustic-wave velocity measurements as a function of pressure with a given symbol representing different locations within one sample at a given pressure. Inset: orientation dependence of sound velocities in argon at $4.0(\pm 0.2)$ GPa with chi indicating the angle of rotation about the pressure-loading axis of the diamond cell.

tion distributions (including texturing) of crystals in the sample, as confirmed by x-ray diffraction. Multiple or broad Brillouin peaks also indicate that many crystal orientations are being probed in our measurements (Fig. 1), as does the irregular chi dependence that we observe (Fig. 3, inset).

Our longitudinal velocities fall between the maximum values of Shimizu *et al.*,¹¹ measurements and the minimum values from Grimsditch *et al.*¹⁰ (using our corrected values of refractive index), and are generally consistent with both studies (Fig. 4). At pressures below ~ 10 GPa, the transverse acoustic velocity increases with increasing pressure; however, we observe a weaker pressure dependence in the 10–30 GPa range than did Shimizu *et al.*¹¹ This difference may be attributed to different textures or grain sizes developed in the two studies. We note that the intensity of the shear mode varies significantly from one run to the next and this peak is sometimes not observed (consistent with the zero-pressure elasto-optical coefficients of fcc Ar determined at low temperature).^{20,21}

We derive the average isotropic elastic moduli from the measured longitudinal (V_P) and transverse (V_S) wave velocities by

$$K_s = \rho(V_P^2 - 4V_S^2/3), \quad (1)$$

$$G = \rho V_S^2, \quad (2)$$

where ρ , K_s , and G are the mass density, adiabatic bulk modulus, and shear modulus, respectively. The isothermal bulk modulus $K_T = \rho(dP/d\rho)_T$ is independently determined from high-pressure x-ray diffraction measurements and is related to the adiabatic bulk modulus by

$$K_s = (C_p/C_v)K_T = \rho(C_p/C_v)(dP/d\rho), \quad (3)$$

where C_p/C_v is the ratio of specific heats at constant pressure and constant volume. Using Shimizu, *et al.*'s¹¹ pressure de-

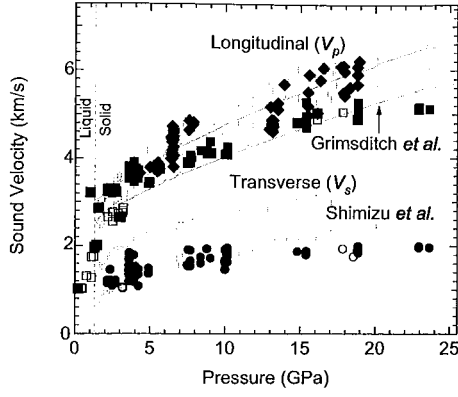


FIG. 4. Longitudinal (upper part) and transverse (lower part) sound velocities of argon as a function of pressure. Closed black symbols denote measurements on compression, and open symbols are on decompression (velocity uncertainty is $\sim 2\%$, smaller than the symbol size, and pressure uncertainty is 0.2–0.7 GPa over the measured range); diamonds and squares correspond to different runs. At 2 GPa our measured V_p and V_s are ~ 3.228 and ~ 1.153 km/s, respectively. Grey crosses and dashed lines indicate the maximum and minima values of sound velocities reported by Shimizu *et al.* (V_p : 2.747–3.239 km/s, V_s : 0.938–1.750 km/s at 2 GPa) (Ref. 11) and Grimsditch *et al.* (V_p : 2.651–3.006 km/s at 2 GPa) (Ref. 10), respectively. The sound velocities of Grimsditch *et al.* are updated here with the refractive index values of the present study.

pendence for this ratio, Eqs. (1)–(3) give the isothermal compression

$$dp/dP = (C_p/C_v)/(V_p^2 - 4V_s^2/3). \quad (4)$$

Integrating with respect to pressure (done numerically and requiring a few iterations), we find $C_p/C_v = 1 + 0.25(\pm 0.11)\exp[-0.197(\pm 0.041) \cdot P]$, assuming a functional form that has been used previously,^{11,22} and determine the pressure dependence of density shown in Fig. 5. Fitting an Eulerian finite-strain (Birch-Murnaghan) equation of state to this result,^{23,24} we obtain $K_T = 15.1(\pm 1.1)$ GPa and $K'_T = 5.4(\pm 0.3)$ for the isothermal bulk modulus and its pressure derivative at 2 GPa and room temperature (Table I; density of 2.18 ± 0.06 g/cm³). Our extrapolated value for the zero-

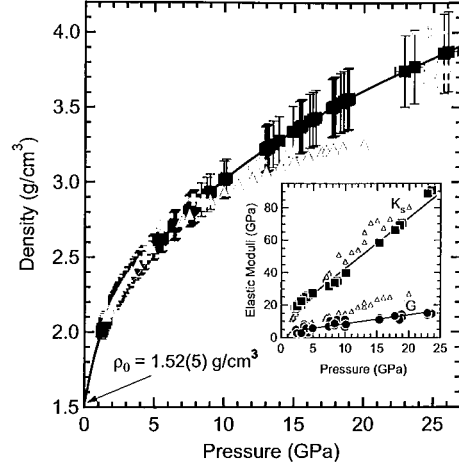


FIG. 5. Equation of state of fcc argon, fitted using the Birch-Murnaghan equation (solid line). Black squares are densities calculated by integrating K/ρ derived from our V_p and V_s values at a given pressure (and two different angles to correct for index of refraction), including the correction from adiabatic to isothermal modulus (see text). A density of 2.02 g/cm³ at 1.3 GPa was used to initiate the integration. Grey triangles represent the results of Shimizu *et al.* (Ref. 11). Grey crosses denote the density measured by x-ray diffraction (Ref. 25). Inset: bulk and shear moduli of polycrystalline fcc argon with lines showing linear fits to the data. K_s and G from Shimizu *et al.* (Ref. 11) are also shown as grey triangles.

pressure density, $1.52(\pm 0.05)$ g/cm³, is consistent with the room-temperature density of 1.564 g/cm³ estimated from low-temperature measurements on fcc argon at zero pressure.²²

The room-temperature isotherm obtained from our Brillouin measurements agrees well with the x-ray diffraction results of Ross *et al.*²⁵ (Fig. 5), which—in turn—are consistent with more recent measurements at higher pressures.⁶ Our equation of state parameters (density, bulk modulus, and pressure derivative) are also compatible with the values obtained from the x-ray diffraction studies, given estimated uncertainties (Table I). As we did not use the x-ray diffraction results to constrain the pressure dependence of density, this agreement between independent experiments illustrates the

TABLE I. Elastic constants (in GPa) of fcc argon at 2 GPa and 290 K.

	K_s	dK_s/dP	G	dG/dP	K_T	dK_T/dP
Theoretical ^a	16.4	4.4	3.7	0.5	16.4	4.4
Grimsditch <i>et al.</i>	11 ± 1.0	4.9 ± 0.5	3.8 ± 0.5	2.4 ± 0.04	11 ± 1.0	4.9 ± 0.5
Shimizu <i>et al.</i> ^b	14.3 ± 1.5	4.1 ± 0.4	4.2 ± 0.4	1.4 ± 0.04	12.3 ± 1.5	4.2 ± 0.4
This study	17.6 ± 1.4	5.1 ± 0.3	4.1 ± 0.4	0.6 ± 0.05	15.1 ± 1.1	5.4 ± 0.3
Ross <i>et al.</i> ^c					14.1 ± 1.0	6.0 ± 0.3
Errandonea <i>et al.</i> ^d					16.7 ± 0.5	5.1 ± 0.3

^aBased on fits to the values in Table III of Ref. 10.

^bEstimated from Fig. 3 of Ref. 11.

^cBased on a Birch-Murnaghan equation fit to the data listed in Table I of Ref. 25.

^dExtrapolated from the zero-pressure bulk modulus in Ref. 6.

utility of high-pressure Brillouin scattering for characterizing the elasticity of polycrystalline materials despite the scatter caused by orientation-dependent velocities.

Our results place constraints on the second pressure derivative of the bulk modulus, given the good agreement of our third-order Eulerian finite-strain equation of state with the x-ray data.^{23,24} Specifically, the nondimensional product $K_T K_T'' = -7.3(\pm 1.2)$ at 2 GPa; along our value for K_T' , this reinforces Birch's point that despite the bulk modulus of various crystals spanning several orders of magnitude, it is remarkable that the (nondimensional) pressure derivatives are found to lie within limited ranges, $4 \leq K_T' \leq 8$ and $-15 \leq K_T K_T'' \leq -4$.²³ To our knowledge, there is as yet no theoretical explanation for this empirical finding.

The bulk and shear moduli as functions of pressure are determined from Eqs. (1) and (2) (Fig. 5 inset). Using these values of G , the 300 K shear strength of crystalline argon can be obtained as a function of pressure from Eq. 5 of Ref. 12 and the differential strains measured in that study. Evidently, fcc Ar exhibits an increase in strength at pressures above 10–12 GPa, albeit with values remaining well below the theoretical limits on yield strength (Fig. 6).²⁶ It is not obvious that the observed increase in strength is uniquely related to pressure, however, as shear-stress-induced dislocations could play a role in the hardening of argon: the density of dislocations can increase rapidly under nonhydrostatic loading, in a manner analogous to cold working of metals.²⁷ Still, our values of shear strength suggest that Ar can be considered a useful medium for quasihydrostatic experiments to at least 30 GPa, especially with thermal annealing.

IV. SUMMARY

We have determined the elastic moduli, shear strength, equation of state, and refractive index of polycrystalline argon from 1.3 to 30 GPa at room temperature by using 180° and 70° Brillouin scattering in a diamond-anvil cell. These results, obtained without using the x-ray diffraction results to constrain the pressure dependence of density, are compared with previously reported studies. The resulting equation of state agrees well with previous x-ray diffraction measure-

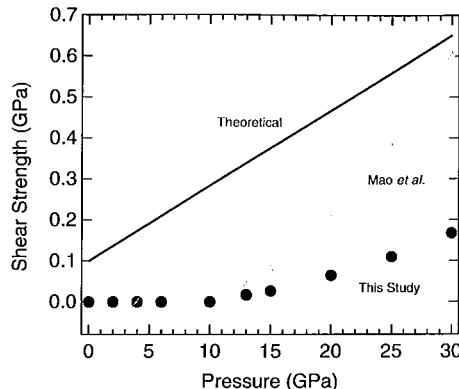


FIG. 6. Shear strength of solid argon at high pressures derived from the measurements of Mao *et al.* (Ref. 12) using our values of G (solid circles), compared with the values of strength given in Ref. 12. The solid line indicates the theoretical limit to shear strength (Ref. 26).

ments, illustrating the suitability of high-pressure Brillouin scattering for characterizing the elasticity and strength of polycrystalline materials.

ACKNOWLEDGMENTS

Financial support for this work was provided by the Consortium for Materials Properties Research in Earth Sciences (COMPRES), the National Science Foundation and Department of Energy, including funding for A. E. Gleason (Carnegie/DOE Alliance Center for High Pressure Science and Technology) and support for the Advanced Light Source (DOE under Contract No. DE-AC02-05CH11231). The diamond cells used in our study were constructed by G. Rose (Princeton University). We are grateful for assistance from T. Duffy, F. Jiang, and Z. Mao (Princeton University), S. Spziale (German Research Centre for Geosciences, Potsdam), and J. Knight (Lawrence Berkeley National Laboratory). We thank Selva Raju for helpful discussions and H. Shimizu for prereview reading.

*Author to whom correspondence should be addressed; bchen@lbl.gov

¹W. Bassett and E. Brody, in *High-Pressure Research: Applications in Geophysics*, edited by M. H. Manghni and S. Akimoto (Academic Press, New York, 1977), pp. 503–508.

²H. Shimizu and S. Sasaki, *Science* **257**, 514 (1992).

³S. V. Sinogeikin and J. D. Bass, *Geophys. Res. Lett.* **29**, 1017 (2002).

⁴M. Murakami, Y. Asahara, Y. Ohishi, N. Hirao, and K. Hirose, *Phys. Earth Planet. Inter.* **174**, 282 (2009).

⁵R. J. Hemley, P. M. Bell, and H. K. Mao, *Science* **237**, 605 (1987).

⁶D. Errandonea, R. Boehler, S. Japel, M. Mezouar, and L. R. Benedetti, *Phys. Rev. B* **73**, 092106 (2006).

⁷T. Itaka and T. Ebisuzaki, *Phys. Rev. B* **65**, 012103 (2001).

⁸R. B. Stewart and R. T. Jacobsen, *J. Phys. Chem. Ref. Data* **18**, 639 (1989).

⁹R. Jia, F. Li, M. Li, Q. Cui, Z. He, L. Wang, Q. Zhou, T. Cui, G. Zou, Y. Bi, S. Hong, and F. Jing, *J. Chem. Phys.* **129**, 154503 (2008).

¹⁰M. Grimsditch, P. Loubeyre, and A. Polian, *Phys. Rev. B* **33**, 7192 (1986).

¹¹H. Shimizu, H. Tashiro, T. Kume, and S. Sasaki, *Phys. Rev. Lett.* **86**, 4568 (2001).

¹²H. K. Mao, J. Badro, J. Shu, R. J. Hemley, and A. K. Singh, *J. Phys.: Condens. Matter* **18**, S963 (2006).

¹³H. K. Mao, J. Xu, and P. M. Bell, *J. Geophys. Res.* **91**, 4673 (1986).

- ¹⁴H. K. Mao, P. M. Bell, J. W. Shaner, and D. J. Steinberg, *J. Appl. Phys.* **49**, 3276 (1978).
- ¹⁵K. J. Koski and J. L. Yarger, *Appl. Phys. Lett.* **87**, 061903 (2005).
- ¹⁶A. E. Gleason, B. Chen, and R. Jeanloz, *Geophys. Res. Lett.* **36**, L23309 (2009).
- ¹⁷C. H. Whitfield, E. M. Brody, and W. A. Bassett, *Rev. Sci. Instrum.* **47**, 942 (1976).
- ¹⁸S. Sasaki, N. Wada, T. Kume, and H. Shimizu, *J. Raman Spectrosc.* **40**, 121 (2009).
- ¹⁹H. Shimizu, N. Saitoh, and S. Sasaki, *Phys. Rev. B* **57**, 230 (1998).
- ²⁰H. Z. Cummins and P. E. Schoen, in *Laser Handbook*, edited by F. T. Arecchi and E. O. Schultz-Du Bois (North-Holland, Amsterdam, 1971), pp. 1029–1075.
- ²¹Landolt Börnstein, in *Numerical Data and Functional Relationships in Science and Technology*, edited by O. Madelung and W. Martienssen (Springer, New York, 1996).
- ²²B. L. Smith and C. J. Pings, *Physica (Amsterdam)* **29**, 555 (1963).
- ²³F. Birch, *J. Phys. Chem. Solids* **38**, 175 (1977).
- ²⁴F. Birch, *J. Geophys. Res.* **83**, 1257 (1978).
- ²⁵M. Ross, H. K. Mao, P. M. Bell, and J. A. Xu, *J. Chem. Phys.* **85**, 1028 (1986).
- ²⁶W. O. Soboyejo, *Mechanical Properties of Engineered Materials* (Marcel Dekker, New York, 2003), pp. 142–144.
- ²⁷B. Chen, H. Zhang, K. A. Dunphy-Guzman, D. Spagnoli, M. B. Kruger, D. V. S. Muthu, M. Kunz, S. Fakra, J. Z. Hu, Q. Z. Guo, and J. F. Banfield, *Phys. Rev. B* **79**, 125406 (2009).

DISCLAIMER

This document was prepared as an account of work sponsored by the United States Government. While this document is believed to contain correct information, neither the United States Government nor any agency thereof, nor the Regents of the University of California, nor any of their employees, makes any warranty, express or implied, or assumes any legal responsibility for the accuracy, completeness, or usefulness of any information, apparatus, product, or process disclosed, or represents that its use would not infringe privately owned rights. Reference herein to any specific commercial product, process, or service by its trade name, trademark, manufacturer, or otherwise, does not necessarily constitute or imply its endorsement, recommendation, or favoring by the United States Government or any agency thereof, or the Regents of the University of California. The views and opinions of authors expressed herein do not necessarily state or reflect those of the United States Government or any agency thereof or the Regents of the University of California.